Received: June 11, 2022. Revised: August 13, 2022.

International Journal of
Intelligent Engineering & Systems

http://www.inass.org/

Image Improvement via Fuzzy Inference Centered Contextual-Dissimilarity Histogram Equalization

Shimaa Janabi[1]* **Mohammed Hussein Ali[2]**

[1]*Department of Computer Technical Engineering, Faculty of Computer Technical Engineering, Almustafa University College, Baghdad, Iraq*
[2]*Electronic and Communications Engineering, Al-Nahrain University, Baghdad, Iraq*
* Corresponding author Email: shimaa.cte@almustafauniversity.edu.iq

Abstract: To solve the drawbacks of existing picture enhancement methods which include the error that occur in the pixel intensity expression, a fuzzy inference-centered contextual-dissimilarity histogram equalization (FICDHE) approach is suggested. Proposed system has three components. The first module generates intensity membership functions based on predicted intensity intervals. Second, fuzzy inference techniques are constructed and contextual-dissimilarity of every pixel is determined. In the last module, dissimilarity histograms are cut and leveled. The fuzzy system in this study not only addresses the uncertainty source of pixel gray level expression, but is also adaptable. In this approach, the fuzzy inference system membership function parameter is automatically selected depending on picture pixel gray. Its versatility creates an algorithm that is more accessible. Two typical medical photos from BrainWeb are used in experiments. Performance of the suggested technique was compared against a number of enhancement algorithms based on subjective evaluation and picture quality measurement indexes. Experiments show that the proposed method is superior to the other algorithms in terms of improving the contrast improvement index (CII) (03.603), the peak signal-to-noise ratio (PSNR) (22.877), the entropy (E) (06.781), the enhancement measures (EME and EMEE) (56.688 and 3344.63 respectively), the quality index based on local variance (QILV) (00.965), and the feature similarity index (FSIM Index) (00.905).

Keywords: Histogram equalization contextual-dissimilarity, Fuzzy inference system, Contrast enhancement, Probable intensity interval.

1. Introduction

Medical photos include low contrast and narrow gray levels. Image enhancement distinguishes diagnostic signs and aids early detection of diseases. Image enhancement increases local contrast to emphasize features. Contrast algorithms can improve pixel intensity difference, improving visual impression [1]. Most methods involve histogram equalization (HE) and morphological processes [2]. HE is popular since it's simple and practical [3]. HE's biggest downside is over-enhancement and artifacts. To circumvent the constraint and improve outcomes, HE-based algorithms were developed. Some algorithms separate the picture into sub images for HE. Bi-histogram equalization (BBHE) splits the original histogram by the mean [4]. "Dynamic Histogram Equalization" (DHE) uses the histogram's local minimum to separate high-order and low-order components and manage gray stretch to improve picture characteristics [5]. "Brightness Preserving Dynamic HE" (BPDHE) and "Brightness Preserving Dynamic Fuzzy HE" (BPDFHE) splits the histogram at the local highest intensity [6], [7]. Singh et al. [8] suggested a recursive histogram division-based approach using picture exposure based on BPDHE, however it fails to improve photos with extreme high or low brightness. Over-enhancement still happens with these procedures. The "contrast limited adaptive HE" (CLAHE) algorithm redistributes pixels with similar intensity to every level. It enhances contrast well but not subtle details [9]. "Exposure-based Sub Image HE"

(ESIHE) employs an exposure threshold to sub-divide clipped histogram; fusing each sub-image after HE improves contrast [10]. Besides HE-based algorithms, literature includes random search methods. Saitoh et al. [11] used the genetic algorithm (GA) to construct a mapping function that compares the initial and augmented images. The function's value measures enhancement quality. Kamoona et al. [12] suggested an enhanced cuckoo search (ECS) technique to optimize the local/ global enhancement transformation parameters. ECS constructs an objective function using entropy and edge intensities. In most cases, there is no objective function that fits all types of images, which reduces the algorithm's versatility.

Engineering uses fuzzy set and fuzzy systems [13]–[15]. Low contrast images reflect fuzzy pixel intensity, and fuzzy theory is used to boost contrast. Pal et al. [16] converted pixel intensity into a fuzzy set and increased contrast. Jenifer et. al. [17] suggested a fuzzy clipped CLAHE system which employs the "fuzzy inference system" (FIS) to automatically calculate the clip limit. In an identical fashion, the triangular fuzzy membership CLAHE (TFM-CLAHE) algorithm uses the triangular fuzzy membership function to calculate the clip limit [18]. Because the FIS membership function parameters are fixed, the clip limit value is not suitable for some dynamic range photos. Kaur et al. [19] introduced a type II fuzzy set contrast method. This method uses the hamacher T co-norm to improve medical picture quality. It can enhance global brightness and diminish visibility. Huang et al. [7] modified BPDHE by using a fuzzy histogram. The method improves low dynamic range photos but not high dynamic range ones.

Most of these algorithms use global statistics and ignore context. Local histogram equalization (LHE) uses a sliding kernel to acquire intensity information in a local region and conduct HE in each sub-image [20]. LHE may introduce checkerboard artifacts during sub-image fusion. "Fuzzy Contextual Contrast Enhancement" (FCCE) creates a fuzzy dissimilarity histogram from fuzzy contrast factor [21]. The final improved image is based on the fuzzy dissimilarity index and a variant of the original image. "Fuzzy contextual-dissimilarity adaptive histogram equalization" (FCDAHE). This approach calculates the fuzzy clip limit and fuzzy dissimilarity clipped histogram using fuzzy inference. FCDAHE performs better than fuzzy clipped CLAHE but has the same drawbacks. "Fuzzy-based Improved Particle Swarm Optimization" (FIPSO) is utilized to generate optimum values for DHE's cumulative distribution function [22]. Real-world imagery isn't ideal for a variety of reasons. Low contrast may occur. This impacts the observation of picture objects and the discovery of hidden information. Due to imaging apparatus limitations, there may be some fluctuation in pixel intensity expression or noise interference. This imaging ambiguity renders pixel gray levels unclear. Pixel gray level changes near ground truth. All of these contrast enhancement approaches assume precise pixel intensity, which is seldom true. Most of these algorithms have the following flaws: Some image subregions are over- or under-enhanced; fixed parameters in the transform function or FIS membership function need sophisticated computation or subjective selection, reducing flexibility; contrast enhancement employs global-statistics and cannot enhance all image areas; existing algorithms' flaws make it tough to improve results. Existing challenges require an image enhancing approach.

This paper offers a FIS with automated parameters for contextual-dissimilarity assessment, "Fuzzy Inference based Contextual-dissimilarity Histogram Equalization" (FICDHE). This approach considers pixel fuzziness and context. Existing techniques usually presume correct picture pixel expression. The method considers global picture statistics and pixel context to establish a suitable global-local balance. The program breaks the picture into sub images to boost the impact. The improved image has no artifacts or oversaturation, so it's fine. It may totally increase picture contrast and expose buried information, allowing for additional image analysis. FICDHE calculates pixel intensity intervals using linear interpolation. Next, the fuzzy inference system returns pixel dissimilarity. The sub-image dissimilarity histogram is trimmed by an adjustable threshold. The sub-images are combined to create the final picture. The remaining portions are as follows: Section 2 explains FICDHE. Section 3 provides image quality indices. Section 4 describes experimental results, and section 5 concludes.

2. Method

FICDHE has three components. In the initial modules, pixels' intensity interval (II) is interpolated locally. Each sub image's intensity interval may be produced by dividing the image. In the next, FIS is based on interval statistics. FIS's input is the overlapping fraction of surrounding pixels' intensity interval. The FIS membership function is determined by overlapping intensity intervals of neighboring pixels. "Fuzzy contextual-dissimilarity" (FCD) is the result of the established FIS system. In

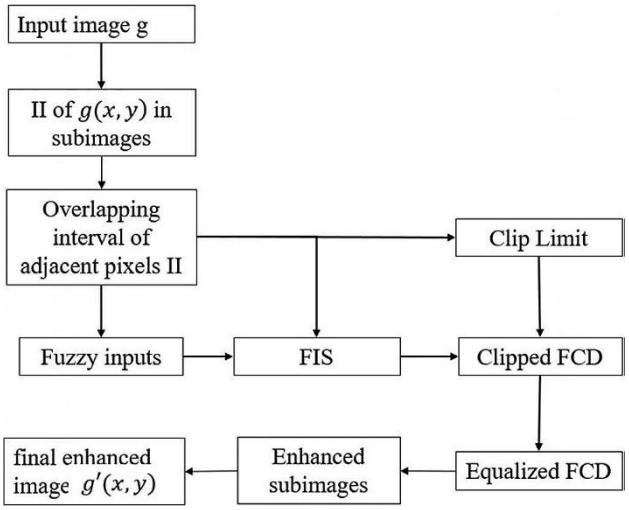

Figure. 1 Framework of FICDHE. FICDHE equalizes fuzzy inference-based contextual dissimilarity histograms

the last module, the clip limit is derived using the overlapping interval statistic to clip the fuzzy contextual-dissimilarity of pixels dissimilarity histogram. After equalizing every histogram, combining the sub-images produces an upgraded picture. Fig. 1 depicts FICDHE's framework.

2.1 Interpixel intensity

Interpolation in the vicinity calculates pixel intensity intervals. Consider a $(M \times N)$ input picture:

$$g = \{g(x,y) | 1 \le x \le M, 1 \le y \le N\} \quad (1)$$

where (x,y) pixel intensity is $g(x,y) = g_k$ and its neighborhood is $N_k(x,y) = \{g(i,j) | x-k \le i \le x+k, y-k \le j \le y+k\}$, where $(k=1)$ for intensity intervals. The middle pixel is the target pixel in the neighborhood, therefore linear interpolation of the intensity in eight directions can calculate its probability interval.

$$\begin{cases} p(x,y) \in [\min(\delta_{zi}), \max(\delta_{zi})] \\ \delta_{zi} = \frac{N_i(x,y) - g(x,y)}{2} + g(x,y) \end{cases} \quad (2)$$

Where $(i = 1, \ldots, 8, p(x,y))$ is the target pixel's interval, and (δ_{zi}) is its' likely intensity. Neighborhood selection requires padding at the image's edge. Because the pixel's uncertainty is mostly in the region with gradual gray-value shift, it won't affect the image's local contrast in the intensity-mutating zone. If the aforementioned approach is employed to construct the interval for the pixel with intensity mutation, excessive measurement of the pixel's gray-value ambiguity will affect histogram equalization. Image mutations are filtered as follows:

$$\bar{\delta}_{zi} = \begin{cases} \max(\delta_{zi}) if\ max(\delta_{zi}) - \alpha g(x,y) < 0 \\ (1+\upsilon) g(x,y)\ if\ \max(\delta_{zi}) - \alpha g(x,y) \ge 0 \end{cases} \quad (3)$$

$$\underline{\delta}_{zi} = \begin{cases} (1-\upsilon) g(x,y)\ if \beta g(x,y) - min(\delta_{zi}) < 0 \\ \min(\delta_{zi})\ if \beta g(x,y) - min(\delta_{zi}) \ge 0 \end{cases} \quad (4)$$

Where $(\bar{\delta}_{zi})$ and $(\underline{\delta}_{zi})$ are the interval's upper and lower bounds respectively. $(\alpha, \beta, \upsilon)$ are constants. Trial-and-error experiments can determine the formula's parameters. In this study, α =1.5, β =0.5, and υ =0.25 are recommended. Traversing all picture pixels yields all possible intensity intervals. $\mu_{p(x,y)}$is the membership function about (δ_{zi}) for the pixel at (x,y). The triangular function is used as its form and mean (δ_{zi}) is regard as its vertex. $\mu_{p(x,y)}(\delta_{zi}, x, y)^{i \in [1,8]}$ can be conveyed as:

$$\mu_{p(x,y)}(\delta_{zi}, x, y) = \begin{cases} \frac{g - \delta_{min}}{\delta_m - \delta_{min}}, g \in [\delta_{min}, \delta_m] \\ \frac{\delta_{max} - g}{\delta_{max} - \delta_m}, g \in [\delta_m, \delta_{max}] \\ \delta_m = \underset{1 \in [1,8]}{\text{mean}}(\delta_{zi}) \end{cases} \quad (5)$$

Instead of the median, the mean of the gray value range is the triangle vertex. Using the median value as the triangle's vertex may result in membership function deviance due to low pixel intensity. When using the mean value, it is less likely to be around the intensity interval's boundary and more likely towards the middle. Comparing the enhancing impact of membership function creation approaches using median value and mean value, testing results reveal that utilizing mean value is superior. Other pixels have the same membership role.

2.2 System of fuzzy inference

The likely intensity intervals are used to produce input for the fuzzy inference system (FIS). The fraction of the overlapping region among the center pixel and the contextual-pixels intensity membership functions may be utilized to assess pixel intensity similarity. We utilized these commonalities as the FIS's input, which may be represented as follows:

$$p_1 = \frac{\mu_{p(x,y)}(\delta_{zi}, x, y) \cup \mu_{p(u,v)}(\delta_{zi}, u, v)}{\min\limits_{i,j \in \{(x,y),(u,v)\}} \Sigma |\mu_{p(i,j)}(\delta_{zi}, i, j)|} \quad (6)$$

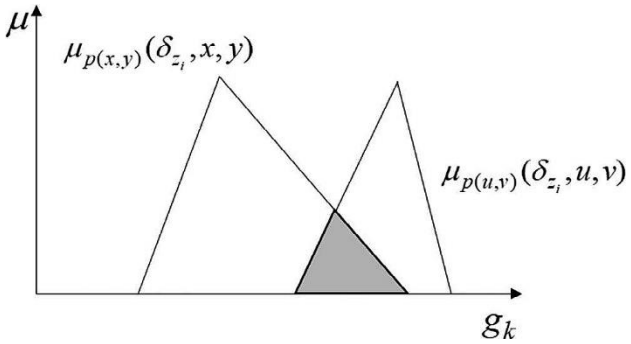

Figure. 2 Common region of two context intervals

$$p_2 = \frac{\mu_{p(x,y)}(\delta_{zi},x,y)\cup\mu_{p(u,v)}(\delta_{zi},u,v)}{\max\limits_{i,j\in\{(x,y),(u,v)\}}\sum|\mu_{p(i,j)}(\delta_{zi},i,j)|} \quad (7)$$

p_1 is the ratio of the two contextual periods' common area to the lower intensity interval, and p_2 to the larger interval. This is shown in Fig. 2.

FIS is used to determine pixel contextual-dissimilarity. A standard rule indicates that; a fuzzifier, an inference engine, and a defuzzifier comprise the FIS [23]. p_1 and p_2 generate input and have three relationships. If (p_1 (max) $\leq p_2$ (min)), then $input_1 = [p_2(min) - p_1(max)]/\Delta(p_1)$ and $input_2 = [p_2(min) - p_1(max)]/\Delta(p_2)$ respectively.

Takagi et al. suggested Mamdani FIS and TSK FIS. In Mamdani FIS, the output is a fuzzy set that must be defuzzified. TSK FIS maps input variables to a clear output. To achieve adaptive picture correction, the FIS parameters described in this research must be calculated based on the intensity interval overlapped region. If TSK FIS is employed, the mapping parameters in each rule must be computed with global statistical information, which increases the computation amount and reduces TSK FIS's benefit. Because TSK FIS is a mixture of function expressions, it cannot handle uncertainty induced by erroneous input data. This paper's input originates from the uncertainty of picture pixel expression, which is created by erroneous pixel expression. This limit TSK FIS. We use Mamdani.

Set the fuzzy rule using the image's pixels that fulfill the previously mentioned requirements. High (H) and low (L) $input_1$ portions. The membership functions are denoted as $G(x,\sigma_{1L},m_{1L})$ and $G(x,\sigma_{1H},m_{1H})$, where:

$$m_{1L} = \min_{i\in I\, j\in I}\left\{abs\left((P_i(min) - P_j(max))\Big/\Delta(P_j)\right)\right\}, \quad j\in neiborhood(i), \sigma_{1L} = m_{IH}/4 \quad (8)$$

$$m_{1H} = \max_{i\in I\, j\in I}\left\{\left((P_i(min) - P_j(max))\Big/\Delta(P_j)\right)\right\}, \quad j\in neiborhood(i), \sigma_{1H} = m_{IH}/4 \quad (9)$$

Due to p_2's scope, $input_2$ is separated into low (L), medium (M), and high (H). Gaussian functions are used as membership functions and are represented as $G(x,\sigma_{2L},m_{2L})$, $G(x,\sigma_{2M},m_{2M})$, and $G(x,\sigma_{2H},m_{2H})$.

$$m_{2L} = \min_{i\in I\, j\in I}\left\{abs\left((P_i(min) - P_j(max))\Big/\Delta(P_i)\right)\right\}, \quad j\in neiborhood(i), \sigma_{2L} = m_{2H}/5 \quad (10)$$

$$m_{2M} = m_{2L} + {}^{(m_{2H}-m_{2L})}/_{2,}\ \sigma_{2M} = {}^{m_{2M}}/_{5} \quad (11)$$

$$m_{2H} = \max_{i\in I\, j\in I}\left\{\left((P_i(min) - P_j(max))\Big/\Delta(P_i)\right)\right\}, \quad j\in neiborhood(i), \sigma_{2H} = m_{2H}/5 \quad (12)$$

Output is pixel similarity. Similarity is $[0,1]$. Low (L), medium (M), and high (H) production are categorized. $G(x,0.15,0)$, $G(x,0.1,0.5)$, and $G(x,0.15,1)$ are Gaussian membership functions. The fuzzy rules employ the Mamdani implication [24].

- If both $input_1$ *and* $input_2$ are L, the result is L.
- Output is M if $input_1$ is H and $input_2$is M.
- If both inputs are H, the result is H.

Multiple rules are combined using minimal (T) norm. Fig. 3 shows Mamdani's FIS.

The defuzzifier uses a centroid defuzzifier as shown:

$$\begin{cases} s(X') = \\ \frac{\sum_{l=1}^{3} cos(G^l) f^l(X')}{\sum_{l=1}^{3} f^l(X')} = \frac{\sum_{l=1}^{3} c^l f^l(X')}{\sum_{l=1}^{3} f^l(X')} \\ f^l(X') = \\ T_{i=1}^{2} f^l(x_i') = T_{i=1}^{2} \mu_{Q_i^l}\left(X_{i,max}^l \middle| X_i^l\right) \end{cases} \quad (13)$$

$s(x,y) = 0$ if $p_1(min) \geq p_2(max)$ or $p_1(max) < p_2(min)$, meaning intensity intervals don't overlap. If $p_1(min) \leq p_2(min)$ and $p_1(min) < p_2(max)$, then $s(x,y) = 1$. The target pixel's intensity similarity to neighboring pixels can also be determined.

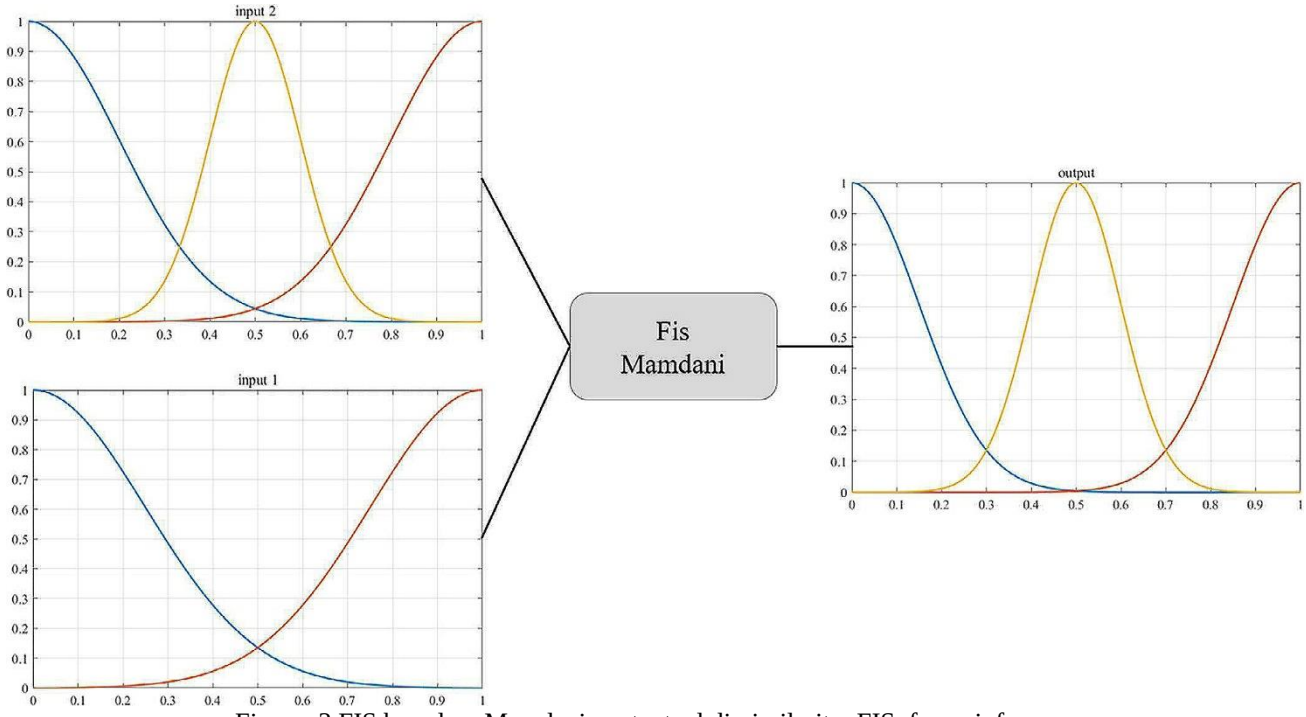

Figure. 3 FIS based on Mamdani contextual dissimilarity. FIS, fuzzy inference

$$s(x,y) = \frac{1}{8}\sum_{i\in\{-1,1\}}\sum_{j\in\{-1,1\}} output(x+i, y+j) \quad (14)$$

$dis(x,y) = \bar{s}(x,y)$ expresses the fuzzy contextual-dissimilarity between the target and neighboring pixels. By traversing all the pixels in a full picture, we may generate the fuzzy contextual-dissimilarity histogram H_{fdis}. The picture is broken into U- and V-shaped blocks. Fuzzy dissimilarity histograms are created for each sub image as follows:

$$H_{fdis}^{ij} = \{h_{fdis}(g_k) | k \in [0, L-1]\}, i = 1, \dots, u; j = 1, \dots, v \quad (15)$$

$$h_{fdis}^{ij}(g_k) = \sum_{x=0}^{M}\sum_{y=0}^{N} u_{gk}(x,y), i = 1, \dots, u; j = 1, \dots, v \quad (16)$$

$$u_{gk}(x,y) = \begin{cases} dis(x,y) \; if \; g(x,y) = g_k \\ 0 \; others \end{cases} \quad (17)$$

2.3 Equalization and fusion of clip limit histograms

Histogram equalization employs statistical information from each sub image's fuzzy contextual-dissimilarity histogram. Because straight equalization of the fuzzy contextual-dissimilarity histogram of sub-images may produce local over enhancement, the maximum sub-image enhancement degree is regulated by adding the contrast limit threshold, and the clip limit is computed as follows:

$$clip\ limit = \frac{\max(N) + avg(N)}{2} \quad (18)$$

$Max(N)$ is the maximum fuzzy contextual-dissimilarity histogram and $avg(N)$ is its average. Fuzzy contextual-dissimilarity probability density, $P_{fdis}^{ij}(g_k)$, is determined by:

$$P_{fdis}^{ij}(g_k) = h_{fdis}^{ij}(g_k) / \sum_{k=0}^{L-1} h_{fdis}^{ij}(g_k) \quad (19)$$

From, $P_{fdis}^{ij}(g_k)$, the cumulative distribution function (CDF) is:

$$C_{fdis}^{ij}(g_k) = \sum_{j=0}^{k} P_{fdis}^{ij}(g_k) \quad (20)$$

Like the histogram equalization procedure, it may directly balance the probability density superposition function to yield the improved picture $E = \{E(x,y) | 0 \le x \le M-1, 0 \le Y \le N-1\}$. Its histogram can be represented as:

$$g_k' = g_0' + C_{fdis}^{ij}(g_k')(g_{L-1}' - g_0') \quad (21)$$

where g_k' is sub-image intensity. To eradicate the seam in sub-image block splicing and save improved picture information at the seam, the sub-image blocks are separated with some overlap, and

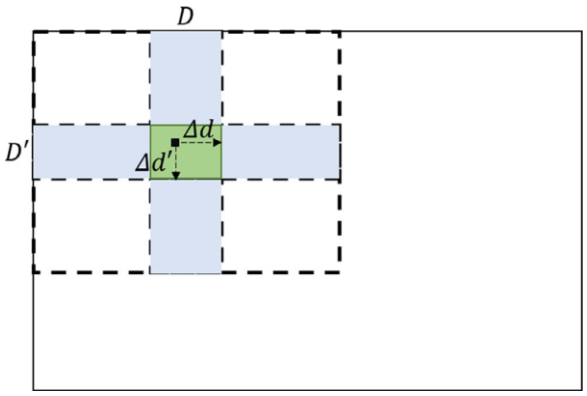

Figure. 4 Subimage splicing diagram. Blue and green overlapping sub-image blocks depict one-time and two-time fusion, respectively

the overlapping portions are weighted fused. Consider two neighboring left and right sub-images, $RF(x,y)$ and $RL(x,y)$. The formula for updating the overlapping part's gray value is:

$$R(x,y) = \frac{\Delta d}{D} RF(x,y) + \left(1 - \frac{\Delta d}{D}\right) RL(x,y) \quad (22)$$

D is the overlap width between pixel (x,y) and the right boundary of the preceding sub-image is Δd. Upper and lower neighboring picture subsets are fused:

$$R(x,y) = \frac{\Delta d'}{D'} RU(x,y) + \left(1 - \frac{\Delta d'}{D'}\right) RD(x,y) \quad (23)$$

As illustrated in Fig. 4, the final enhanced picture is created by allocating the overlapped fused image component to one of the two sub-images and truncating the overlapping sub-image part.

2.4 Evaluation of image quality

Contrast enhancement algorithm performance is evaluated using quality assessment metrics. Contrast improvement index (CII), peak signal-to-noise ratio (PSNR), entropy (E), enhancement measures (EME and EMEE), quality index based on local variance (QILV), and feature similarity (FSIM) index. These indices and parameters measure picture quality and FICDHE's performance. Contrast improvement index (CII) measures the level of contrast improvement based on the original and improved image's local contrast. Calculating an image's CII [4]:

$$C(I) = \sum_{u,v=0}^{L-1} \delta(u,v)^2 P_\delta(u,v) \quad (24)$$

$$CII = \frac{C(I')}{C(I)} \quad (25)$$

$C(I')$ is the improved image's local contrast and $C(I)$ is the original's. Higher (CII) increases visual contrast. PSNR is used to determine if improved pictures are suitable for consumer electronics [25]. The original picture is $g(x,y)$, and the improved output image is $g'(x,y)$. Calculating PSNR.

$$PSNR(I) = 10\log_{10} \frac{(L-1)^2}{\frac{1}{MXN}\sum_{i=1}^{M}\sum_{y=1}^{N}(g(x,y)-g'(x,y))^2} \quad (26)$$

L=256 for 8-bit grayscale photos. Increasing PSNR improves output image visibility and vice versa. Entropy measures visual information abundance. Entropy increases information. Image entropy =

$$E(I) = \sum_{u,v=0}^{L-1} -\ln\left(P_\delta(u,v)\right) P_\delta(u,v) \quad (27)$$

Where $\delta(u,v) = |g(u) - g(v)|$ represents pixel intensity difference. $P_\delta(u,v)$ is the probability density between neighboring pixels when δ is the intensity difference. Enhancement measures divide the image into sub images without overlapping parts and calculate the maximum and minimum intensities of each subset.

$$EME = \frac{1}{N}\sum 20\log\frac{g_{max}}{g_{min}} \quad (28)$$

N is the sub-image count. EMEE is related to EME and uses entropy.

$$EME = \frac{1}{N}\sum \frac{g_{max}}{g_{min}} 20\log\frac{g_{max}}{g_{min}} \quad (29)$$

Images should be separated into the same amount of sub images when comparing methods. QILV is a local contrast-based image quality index [26]. Sub-images must be created for QILV. Use the Gaussian function to get each block's weighted mean and variance. Weighted sub-image mean and variance are used to compute k.

$$k(g,g') = \frac{\sum_k (\sigma_k^g - \frac{\sum \sigma_k^g}{N})(\sigma_k^{g'} - \frac{\sum \sigma_k^{g'}}{N})}{N-1} \quad (30)$$

Where N represents the number of sub images. σ_k^g and $\sigma_k^{g'}$ are original and improved subimage variances. Image QILV is:

$$QILV = \frac{4k(g,g')\sum_K \sigma_k^g \sum_K \sigma_k^{g'}}{N^2(\frac{\sum \sigma_k^{g^2}}{N} + \frac{\sum \sigma_k^{g'^2}}{N})(\zeta_g^2 + \zeta_{g'}^2)} \quad (31)$$

Higher QILV improves image quality. Feature similarity (FSIM) index rates image quality based on how humans perceive images [27]. Image quality is objectively assessed. Local detail is assessed using phase consistency matrix and image gradient.

$$FSIM = \frac{S_L . PC_m}{PC_m} \quad (32)$$

$PC_m = \max(\mathrm{PC}_1, \mathrm{PC}_2)$ is the original and augmented image's maximum local phase consistency matrix [28].

$$PC(x) = \frac{\sum_j E_{\theta J}(x)}{\varepsilon + \sum_n \sum_j A_{n,} \theta_j(x)} \quad (33)$$

S_L is the similarity mapping matrix between the original and improved images:

$$S_L = S_{PC} S_G = \frac{2PC_1(x)PC_2(x)+T_1}{PC_1^2+PC_2^2+T_1} . \frac{2G_1(x)G_2(x)+T_2}{G_1^2+G_2^2+T_2} \quad (34)$$

T_1 and T_2 are constants that range from 0 to 1. FSIM higher value indicates an improved image quality.

3. Results

Here, we tested medical graphics. FICDHE was compared against fuzzy-based improved particle swarm optimization DHE (FIPSODHE), BPDHE, and several innovative approaches as TFM-CLAHE, FCDAHE, the type II fuzzy enhancement (TIIFE) algorithm, ESIHE, and the enhanced cuckoo search enhancement (ECSE) algorithm. BPDHE, TIIFE, and ESIHE calculation programs were given by their authors. We program other algorithms based on articles. These algorithms' experimental findings were qualitatively and statistically evaluated. Fig. 5 show improved medical photos and gradation histograms.

Fig. 5 shows the MR Lumbar Spine imaging findings of the above-mentioned and suggested methods. This part uses section 2's objective metrics to assess the proposed algorithm and competing approaches. The above-shown photos' objective assessment parameters are determined. Images are 8-bit integer grayscale. Table 1 exhibit quantitative enhancement indices. Each row's maximum value is bolded. 300 medical photos were randomly picked from the BrainWeb simulated dataset to demonstrate the proposed algorithm's performance. The test dataset has 800 photos. Too many photographs make it difficult to illustrate each upgrade in this study.

4. Discussion

4.1 Qualtive assessment

An improved image must be visually evaluated. No objective picture assessment index exists. Visibility may be improved with a higher-quality picture. Subjective evaluation determines improvement and artifacts. Fig. 5 (b) shows FIPSODHE's improved performance. The contrast has been substantially increased, but the original image's dark parts remain dark. The enhancing effects cause the gray distribution to be more consistent and stretch to the complete gray spectrum. Fig. 5 (c) shows that even though the TFM-CLAHE simulation result was visually appealing, the upper-left region was excessively dark and lacked detail. Fig. 5 (d, e) shows BPDHE and FCDAHE's insufficient textural features and lack of blood vessel enlargement in muscle tissue. BPDHE has an inadequate gray-scale range. Fig. 5 (f) shows the TIIFE-enhanced picture. Contrast was increased, but not uniformly. Overly strong light reduced image

Table 1. Objective quantitative MR lumbar image indexes

Index	FIPSODHE	TFM-CLAHE	BPDHE	FCDAHE	TIIHE	ESIHE	ECSE	FICDHE
CII	03.574	02.422	01.004	03.414	01.346	01.502	01.193	03.603
FSIM	00.912	0.822	00.912	00.858	00.912	00.918	00.905	00.905
Entropy	06.546	06.175	05.353	06.327	05.624	05.594	06.043	06.781
QILV	00.965	00.955	00.602	00.946	00.926	00.953	00.884	00.965
EME	57.144	57.282	31.827	53.966	13.891	55.001	16.311	56.688
EMEE	3442.47	3467.22	2626.36	3007.27	88.262	3218.13	103.65	3344.63
PSNR	20.677	21.325	11.865	20.084	14.837	19.702	16.716	22.877

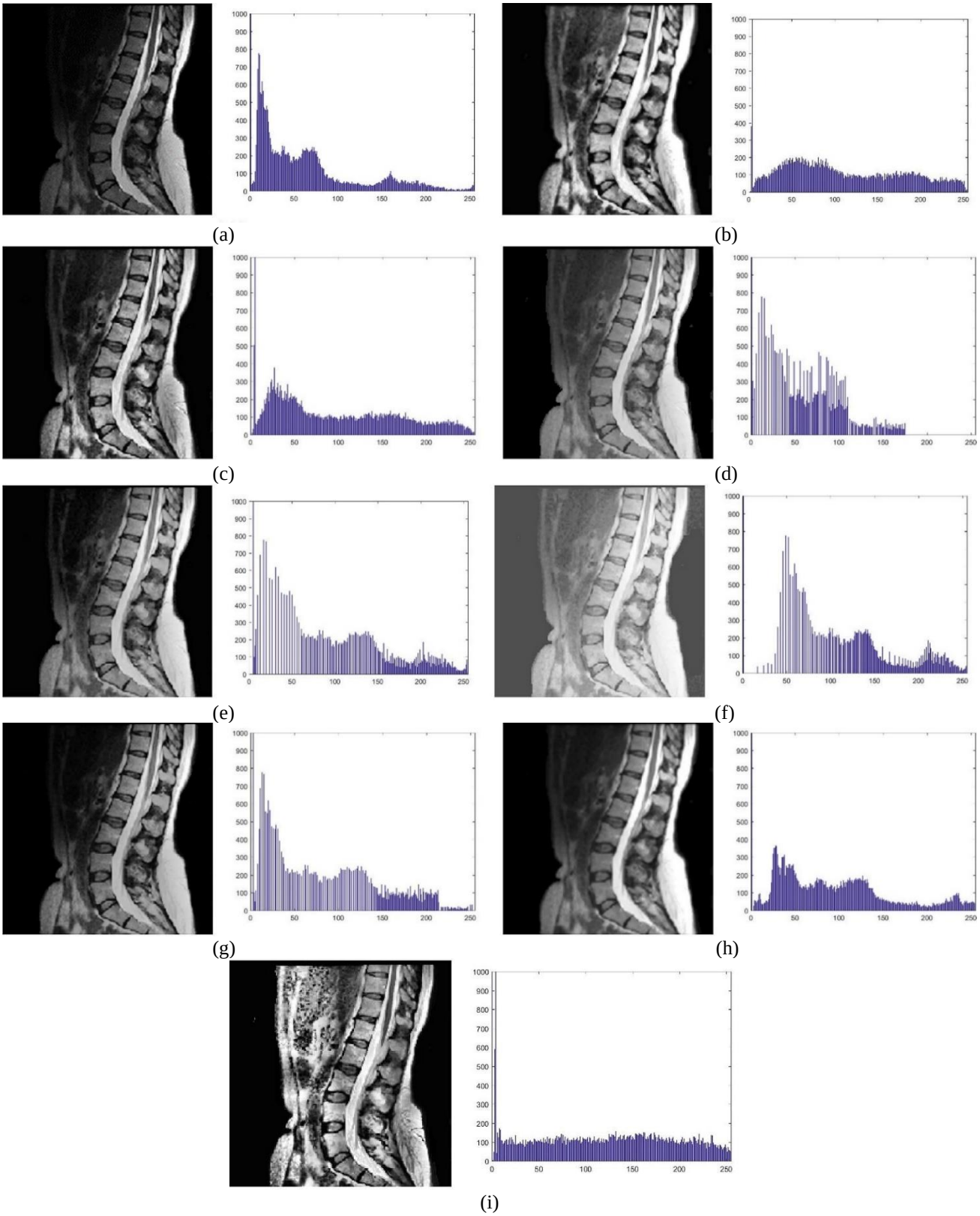

Figure 5. Histograms with MR lumbar spine images. The first row is the original picture and FIPSODHE output. The second row is, TFM-CLAHE output and BPDHE output. The third row is, FCDAHE output and TIIFE output. The fourth row is, ESIHE output and ECSE output. The last image is the FICDHE output

quality. Fig. 5 (g, h) shows decreased texture details and brightness issues. ECE picture quality has degraded. Fig. 5 (i) depicts FICDHE image enhancement. The article's methodology outperformed the others. FICDHE might provide pictures with greater visibility and more low-

contrast detail. Upper left was more contrasty than other regions. Histogram illustrates intensity levels extended over dynamic range.

Two algorithms produced the best enhancements. By subjectively measuring all output outcomes, the suggested technique may increase image quality without adding noise or artifacts. It retains textural features in medical photographs, facilitating diagnosis.

4.2 Quantitive assessment

Noise can impact objective evaluation elements' correctness. In certain circumstances, one index is marginally inferior to others, but that doesn't affect the suggested algorithm's performance. Therefore, you must blend subjective judgment with objective metrics. Most quantitative indexes boosted by the FICDHE algorithm were greater than those of the compared algorithms, while other indexes were similar.

Higher CII implies the algorithm can increase picture contrast more efficiently, and higher entropy indicates FICDHE's outputs are more comprehensive. Higher PSNR suggests that FICDHE didn't add too much noise when improving the picture, while other characteristics reflect superior visual performance. Some picture objective indicators are worse than others. But that doesn't mean this paper's algorithm is bad. Distorted objective index measurement may generate this outcome. The algorithm needs additional photos. Although the enhanced image's entropy isn't as high as TFMCLAHE's, subjective analysis demonstrates that TFM-high CLAHE's entropy is caused by noise. The algorithm's results showed clearer photos. Visibility and picture quality increased greatly. Compared to other methods, FICDHE provides better picture enhancement.

5. Conclusion

Fuzzy inference based contextual dissimilarity histogram equalization (FICDHE) was presented in this research. The algorithm considered intensity uncertainty and generated pixel intensity intervals.

The fuzzy inference system for generating contextual dissimilarity uses the overlapping intervals as input. The contextual dissimilarity histogram compares adjacent pixels. FICDHE selected the clip-limit and avoided over enhancement before equalization. This method smoothed the histogram and preserved the images' brightness and naturalness.

The generated image lacked noise and artifacts. BrainWeb test datasets were used to evaluate the proposed technique qualitatively and quantitatively. Experimental results show that the proposed method enhances dark areas and preserves global brightness. FICDHE enhances contrast locally and globally.

Conflict of interest

The authors declare no potential conflict of interest.

Author contribution

Shimaa Janabi contributed to methodology, software, and writing review and editing, Mohammed Hussein contributed in supervising the overall work and editing the paper.

References

[1] D. Vijayalakshmi, M. K. Nath, and O. P. Acharya, “A comprehensive survey on image contrast enhancement techniques in spatial domain”, *Sensing and Imaging*, Vol. 21, No. 1, pp. 1–40, 2020.

[2] B. Subramani and M. Veluchamy, “Fuzzy contextual inference system for medical image enhancement”, *Measurement*, Vol. 148, p. 106967, 2019.

[3] E. R. Dougherty, *Digital Image Processing Methods*. CRC Press, 2020.

[4] M. Veluchamy, K. Mayathevar, and B. Subramani, “Brightness preserving optimized weighted bi-histogram equalization algorithm and its application to MR brain image segmentation”, *International Journal of Imaging Systems and Technology*, Vol. 29, No. 3, pp. 339–352, 2019.

[5] B. S. Rao, “Dynamic histogram equalization for contrast enhancement for digital images”, *Applied Soft Computing*, Vol. 89, p. 106114, 2020.

[6] P. Kandhway and A. K. Bhandari, “An optimal adaptive thresholding based sub-histogram equalization for brightness preserving image contrast enhancement”, *Multidimens Syst Signal Process*, Vol. 30, No. 4, pp. 1859–1894, 2019.

[7] Z. Huang, Z. Wang, J. Zhang, Q. Li, and Y. Shi, “Image enhancement with the preservation of brightness and structures by employing contrast limited dynamic quadri-histogram equalization”, *Optik (Stuttg)*, Vol. 226, p. 165877, 2021.

[8] N. Singh, L. Kaur, and K. Singh, “Histogram equalization techniques for enhancement of low radiance retinal images for early detection of diabetic retinopathy”, *Engineering Science and*

Technology, an International Journal, Vol. 22, No. 3, pp. 736–745, 2019.

[9] V. Stimper, S. Bauer, R. Ernstorfer, B. Schölkopf, and R. P. Xian, "Multidimensional contrast limited adaptive histogram equalization", *IEEE Access*, Vol. 7, pp. 165437–165447, 2019.

[10] U. K. Acharya and S. Kumar, "Image Enhancement Using Exposure and Standard Deviation-Based Sub-image Histogram Equalization for Night-time Images", In: *Proc. of International Conference on Artificial Intelligence and Applications*, 2021, pp. 607–615.

[11] F. Saitoh, "Image contrast enhancement using genetic algorithm", In: *Proc. 1999 IEEE International Conference on Systems, Man, and Cybernetics (Cat. No. 99CH37028)*, 1999, Vol. 4, pp. 899–904.

[12] A. M. Kamoona and J. C. Patra, "A novel enhanced cuckoo search algorithm for contrast enhancement of gray scale images", *Applied Soft Computing*, Vol. 85, p. 105749, 2019.

[13] Z. Qu and Z. Du, "Interval Type-2 Fuzzy Sampled-Data H∞ Control Under Stochastic Communication", *International Journal of Fuzzy Systems*, Vol. 23, No. 7, pp. 2132–2143, 2021.

[14] Z. Du, Y. Kao, and X. Zhao, "An input delay approach to interval type-2 fuzzy exponential stabilization for nonlinear unreliable networked sampled-data control systems", *IEEE Transactions on Systems, Man, and Cybernetics: Systems*, Vol. 51, No. 6, pp. 3488–3497, 2019.

[15] Z. Du, Y. Kao, and J. H. Park, "New results for sampled-data control of interval type-2 fuzzy nonlinear systems", *J Franklin Inst*, Vol. 357, No. 1, pp. 121–141, 2020.

[16] S. K. Pal, R. King, and others, "Image enhancement using smoothing with fuzzy sets", *IEEE Trans. Sys., Man, and Cyber.*, Vol. 11, No. 7, pp. 494–500, 1981.

[17] S. Jenifer, S. Parasuraman, and A. Kadirvelu, "Contrast enhancement and brightness preserving of digital mammograms using fuzzy clipped contrast-limited adaptive histogram equalization algorithm", *Applied Soft Computing*, Vol. 42, pp. 167–177, 2016.

[18] P. Amsini and R. U. Rani, "Enhanced Type 2 Triangular Intuitionistic Fuzzy C Means Clustering Algorithm for Breast Cancer Histopathology Images", In: *Proc. of 2020 Fourth International Conference on Computing Methodologies and Communication (ICCMC)*, 2020, pp. 589–594.

[19] P. Kaur and T. Chaira, "A novel fuzzy approach for segmenting medical images", *Soft Computing*, Vol. 25, No. 5, pp. 3565–3575, 2021.

[20] V. Stimper, S. Bauer, R. Ernstorfer, B. Schölkopf, and R. P. Xian, "Multidimensional contrast limited adaptive histogram equalization", *IEEE Access*, Vol. 7, pp. 165437–165447, 2019.

[21] S. Li, J. Lu, L. Cheng, and X. Li, "Fuzzy inference based contextual dissimilarity histogram equalization algorithm for image enhancement", *International Journal of Imaging Systems and Technology*, Vol. 31, No. 2, pp. 609–626, 2021.

[22] B. S. Rao, "Dynamic histogram equalization for contrast enhancement for digital images", *Applied Soft Computing*, Vol. 89, p. 106114, 2020.

[23] M. M. JERRY, *Uncertain Rule-Based Fuzzy Systems: Introduction and New Directions*. Springer, 2019.

[24] J. M. Mendel, "Fuzzy logic systems for engineering: a tutorial", In: *Proc. of the IEEE*, Vol. 83, No. 3, pp. 345–377, 1995.

[25] P. W. Jones and M. Rabbani, "Digital image compression", *Digital Image Processing Methods*, pp. 261–325, 2020.

[26] K. Ding, K. Ma, S. Wang, and E. P. Simoncelli, "Image quality assessment: Unifying structure and texture similarity", *ArXiv Preprint ArXiv:2004.07728*, 2020.

[27] U. Sara, M. Akter, and M. S. Uddin, "Image quality assessment through FSIM, SSIM, MSE and PSNR—a comparative study", *Journal of Computer and Communications*, Vol. 7, No. 3, pp. 8–18, 2019.

[28] X. Miao, H. Chu, H. Liu, Y. Yang, and X. Li, "Quality assessment of images with multiple distortions based on phase congruency and gradient magnitude", *Signal Processing: Image Communication*, Vol. 79, pp. 54–62, 2019.